

Morphological and Structural Development of Recycled Crosslinked Polyethylene During Solid-State Mechanochemical Milling

Hejun Wu, Mei Liang, Canhui Lu

State Key Laboratory of Polymer Materials Engineering, Polymer Research Institute of Sichuan University, Chengdu, 610065, China

Received 24 July 2010; accepted 30 November 2010

DOI 10.1002/app.33863

Published online 21 April 2011 in Wiley Online Library (wileyonlinelibrary.com).

ABSTRACT: Waste crosslinked polyethylene (XLPE) was partially decrosslinked to obtain a thermoplastic recycled material through solid-state mechanochemical milling with pan-mill equipment at ambient temperature. The gel fraction and size exclusion chromatography measurements showed that the gel content of XLPE decreased remarkably with increasing cycles of mechanochemical milling, whereas the molecular weight of the sol fraction was not significantly reduced; this indicated the realization of partial decrosslinking during mechanochemical milling. Differential scanning calorimetry and X-ray diffraction analysis showed that the melting temperature of decrosslinked polyethylene increased by 3.5°C because the bigger crystallites size resulting from

the higher mobility of the chain segment. The improved thermoplastic characteristic of XLPE after mechanochemical milling were confirmed by scanning electron microscopy and rheological measurement. The mechanical properties of recycled XLPE also achieved significant improvement after mechanochemical milling. Solid-state mechanochemical milling is a cost-effective, reliable, and environmentally friendly method for recycling XLPE at ambient temperature without any additional materials or chemicals. © 2011 Wiley Periodicals, Inc. *J Appl Polym Sci* 122: 257–264, 2011

Key words: polyethylene (PE); recycling; structure–property relations; thermosets; waste

INTRODUCTION

Crosslinked polyethylene (XLPE) is widely applied for cable insulation because of several of its desirable properties, including low heat transfer and poor conductivity caused by crosslinking.¹ Unfortunately, crosslinking, which can be initiated with peroxides,² by irradiation,³ or by the addition of silanes,⁴ also makes polyethylene (PE) into a thermoset resin. It is difficult to recycle XLPE because of its low fluidity and poor moldability. As the country updates its electrical infrastructure, waste XLPE from scrap power transmission and distribution cables is becoming a significant disposal concern.

The conventional solution for handling waste XLPE is landfills or incineration. However, landfilling requires dedicated land and may lead to soil contamination, and incineration is expensive and

can produce toxic gases.^{5–7} To achieve an environmentally friendly society, the development of more effective recycling technologies is desired. Techniques that have been used to recycle XLPE include conversion into oil by thermal and catalytic cracking^{8,9} and its use as a powdery filler by mixture with thermoplastics in an extruder to make a thermoplastic recycled polymer.¹⁰ Thermal and catalytic cracking is usually carried out at high temperatures and is usually accompanied by a large amount of energy consumption.¹¹ The poor mechanical properties caused by random decomposition of the polymer chain during extrusion also limit the applications of powdered XLPE as a filler.¹²

Although selective decrosslinking at crosslinking points is difficult in conventional methods, the decrosslinking of XLPE remains the most desirable method, as it requires the least energy. Supercritical fluids such as water, methanol, and alcohol are used to obtain high-quality recycled materials through selective decrosslinking at the crosslinking points of XLPE. Watanabe et al.¹³ observed that peroxide-crosslinked PE was selectively decrosslinked without the severe decomposition of backbone chains with supercritical water. Hong et al.¹⁴ studied the decrosslinking of PE in supercritical methanol and confirmed that the molecular weight of the decrosslinked PE was only slightly smaller than that of raw PE. Goto and Yamazaki¹⁵

Correspondence to: C. Lu (canhuilu@263.net) and M. liang (liangmeiww@163.com).

Contract grant sponsor: National Natural Science Foundation of China; contract grant number: 50903053.

Contract grant sponsor: Applied Basic Research Programs of Science and Technology Commission Foundation of Sichuan Province, China; contract grant number: 2010JY0022.

achieved the successful decrosslinking of silane-crosslinked PE in various supercritical alcohols. However, problems still persist because the critical temperature and pressure of these supercritical fluids are high;¹⁶ this is related to the high cost of equipment and difficulty for continuous processing. It remains a technological challenge to develop a more effective method for recycling XLPE without any additional materials and chemicals at ambient temperature.

In recent years, it has been demonstrated that mechanochemical technology has many advantages over other conventional chemical methods in solid waste disposal, such as rubber and plastic recycling, and it has attracted a lot of interest.¹⁷ In this study, we used a cost-effective, reliable, and environmentally sound approach to obtain a thermoplastic recycled material by breaking down the crosslinked structure of XLPE through solid-state mechanochemical milling with pan-mill equipment.^{18,19} The pan-mill equipment was designed in the authors' laboratory for solid-state mechanochemical reactions of polymers, showing multifunctions, such as pulverizing, dispersion, mixing, and activation.^{20–25} Our previous studies^{26–28} have demonstrated that the pan-mill could also be successfully applied to the devulcanization of rubber vulcanizates. The application of solid-state mechanochemical milling to decrosslinked PE was examined in this study. Gel fraction and size exclusion chromatography (SEC) measurements were used to investigate the breakage of the crosslinked structure and the molecular weight change of the gel fraction for XLPE during mechanochemical milling. Further development of the structure and properties of the recycled XLPE was characterized by scanning electron microscopy (SEM), thermogravimetric analysis (TGA), differential scanning calorimetry (DSC) and X-ray diffraction (XRD), respectively. The rheological behavior and mechanical properties of the recycled XLPE were investigated as well.

EXPERIMENTAL

Materials

The cable insulator made from peroxide-crosslinked PE with a crosslinking degree or gel content of 0.70 was supplied by Guangdong NANyang Cable Group Holding Co., Ltd. (Shantou, Guangdong, China). Analytical-reagent-grade xylene, the chemical for gel content determination, was commercially available and was used without further purification.

Mechanochemical milling equipment and process

Figure 1 shows a digital photograph of the equipment and structure of the milling pan. A chain-transmission system and a screw-pressure system

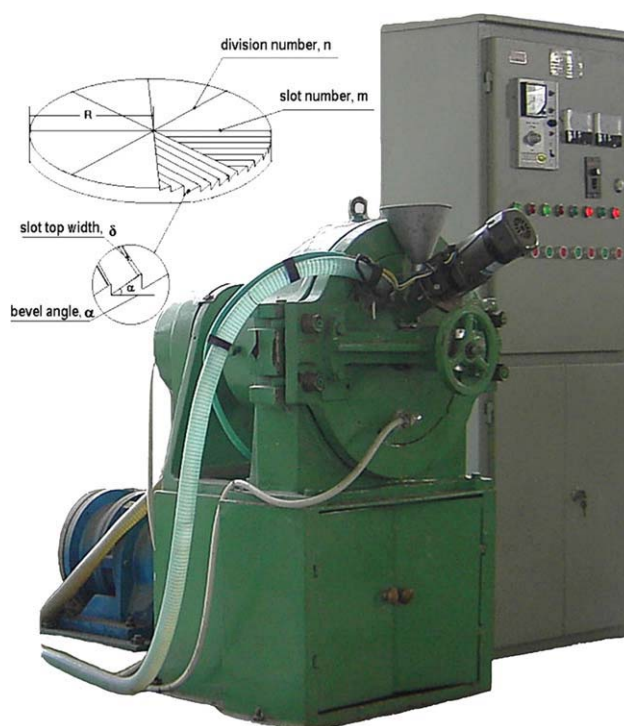


Figure 1 Digital camera picture of the pan-mill-type mechanochemical reactor and schematic diagram of the inlaid milling pan. [Color figure can be viewed in the online issue, which is available at wileyonlinelibrary.com.]

were set to regulate the rotation speed of the moving pan and imposed load, respectively, which could strictly control two major dynamic parameters, the velocity and force during milling. Cooling water flowed through the hollow interior of the pan to take away the heat generated during milling; through the control of the flow, the milling temperature was adjustable.

The decrosslinking of XLPE was carried out in the pan-mill type mechanochemical reactor at ambient temperature. The chips of XLPE were fed into the mechanochemical reactor through the hopper in the center of the milling pan at a rotating speed of 30 rev/min. The milling process of the solid mass in the equipment was as follows: the materials were fed into the center of the pan from the inlet and driven by shear force, moving along a spiral route toward the edge of the pan until they came out from the outlet; this completed one cycle of milling. The discharged powder was collected for the next cycle of milling. The average retention time of the powders during milling was 25–40 s per cycle, and the heat generated during milling was removed by water circulation. The chain-transmission system and a screw-pressure system were set to regulate the rotation speed of the moving pan and imposed load, respectively, which could strictly control two major dynamic parameters during milling: the velocity and force. The repetition operation continued for various

numbers of cycles to produce recycled XLPE. The partially decrosslinked samples of various cycles of milling were collected for further measurements.

Morphological observation

The morphology of XLPE before and after solid-state mechanochemical milling was observed under a scanning electron microscope (SEM; JSM-5600, JOEL, Tokyo, Japan). A thin layer of Pd–Au alloy was coated on the specimen to prevent charging on the surface. SEM observation was operated at 20 kV.

Gel fraction measurements

The gel content of the recycled XLPE was determined gravimetrically according to ASTM D 2765 with a 24-h Soxhlet extraction with xylene as the solvent. The specimens (ca. 0.5 g) were accurately weighed (M_i) and placed in filter paper and then extracted by xylene for 24 h. The rest of the extraction was taken out from the xylene and dried at 80°C under vacuum aspiration for 16 h, so that the solvent would vaporize completely. Then, the insoluble part (M) was obtained and also measured. The gel fraction was calculated from the weight of the specimen before and after abstraction with the following equation, and each sample was measured three times:

$$\text{Gel fraction} = \frac{M}{M_i} \times 100\% \quad (1)$$

SEC measurement

The molecular weight distribution and polydispersity index (PDI) were estimated by SEC at 160°C with 1,2,4-trichlorobenzene as a solvent and narrow-molecular-weight-distribution polystyrene standard samples as references. The measurements were performed on a gel permeation chromatography analyzer (GPC; PL-GPC220, SEC Instruments, Church Stretton, UK) with MIX-C \times 2 columns and a refractive-index detector.

TGA

The thermal stability of XLPE before and after solid-state mechanochemical milling was measured by a thermogravimetric analyzer (TGA; Q600, TA Instruments, New Castle, DE, USA) at a heating rate of 10°C/min from 50 to 550°C. The atmosphere used was nitrogen with a flow rate of 20 mL/min. Approximately 4 mg of each sample was used, and then, thermogravimetric experiments were run in the conditions described previously.

DSC analysis

Small pieces of approximately 5 mg were used to measure the melting temperature (T_m) by using a differen-

tial scanning calorimeter (DSC; DSC-204, Netzsch, Germany). The measurement was carried out under nitrogen at a flow rate of 20 mL/min at 10°C/min scan rate from 40 to 200°C. The T_m 's and the heats of fusion (ΔH_m 's) were evaluated from the peak temperatures and the areas of the maxima of the appropriate endotherms. The crystallinity index ($X_{c,D}$) was calculated by comparison of the measured ΔH_m 's with the melting enthalpy of an infinite size PE orthorhombic crystal ($\Delta H_m^0 = 288 \text{ J/g}$).²⁹ The lamellar thickness (l_c) was determined from the DSC curve with the Thomson–Gibbs equation:

$$T_m = T_m^0(1 - 2\delta_e/\Delta H_m^0 l_c) \quad (2)$$

where T_m^0 is the equilibrium melting point of an infinite PE crystal (414.5 K), ΔH_m^0 is the enthalpy of fusion per unit volume ($288 \times 10^6 \text{ J/m}^3$), δ_e is the surface energy of a PE crystal ($70 \times 10^{-3} \text{ J/m}^2$), and l_c is the thickness of the lamellae with T_m .³⁰

XRD analysis

XRD measurements were performed in a X'Pert X-diffractometer (XRD; Philips Analytical BV, Almelo, The Netherlands) with Cu K α radiation at $\lambda = 0.1540 \text{ nm}$ (40 kV, 40 mA). The degree of crystallinity ($X_{c,R}$) was obtained by resolution of the XRD patterns for the range $5^\circ < \text{Diffraction angle } (2\theta) < 50^\circ$ into the diffraction area relative to the crystalline peaks (I_c) and relative to the amorphous halo (I_a):

$$X_{c,R} = \frac{I_c}{(I_c + I_a)} \times 100\% \quad (3)$$

The strongest lattice plane index (hkl) reflections, (110), (200), and (020), in the applied 2θ range were used as indicators for the determination of the crystallite size (D_{hkl}) by application of the Scherrer equation [eq. (4)], with FWHM_{hkl} as the full width at half-maximum of the hkl reflection:

$$D_{hkl} = \frac{\lambda}{\text{FWHM}_{hkl} \cos \theta_{hkl}} \quad (4)$$

In this simple manner, the influence of any crystal distortion on the full width at half-maximum (fwhm) was neglected. Therefore, the derived data D_{hkl} was of minimum size.³¹

Rheological measurements

The rheological measurements were done in a capillary rheometer (Rheograph 2002, Gottfert, Germany) at different plunger speeds. The plunger speed was varied from 0.06 to 20 cm/min. The melt was extruded through the capillary at predetermined

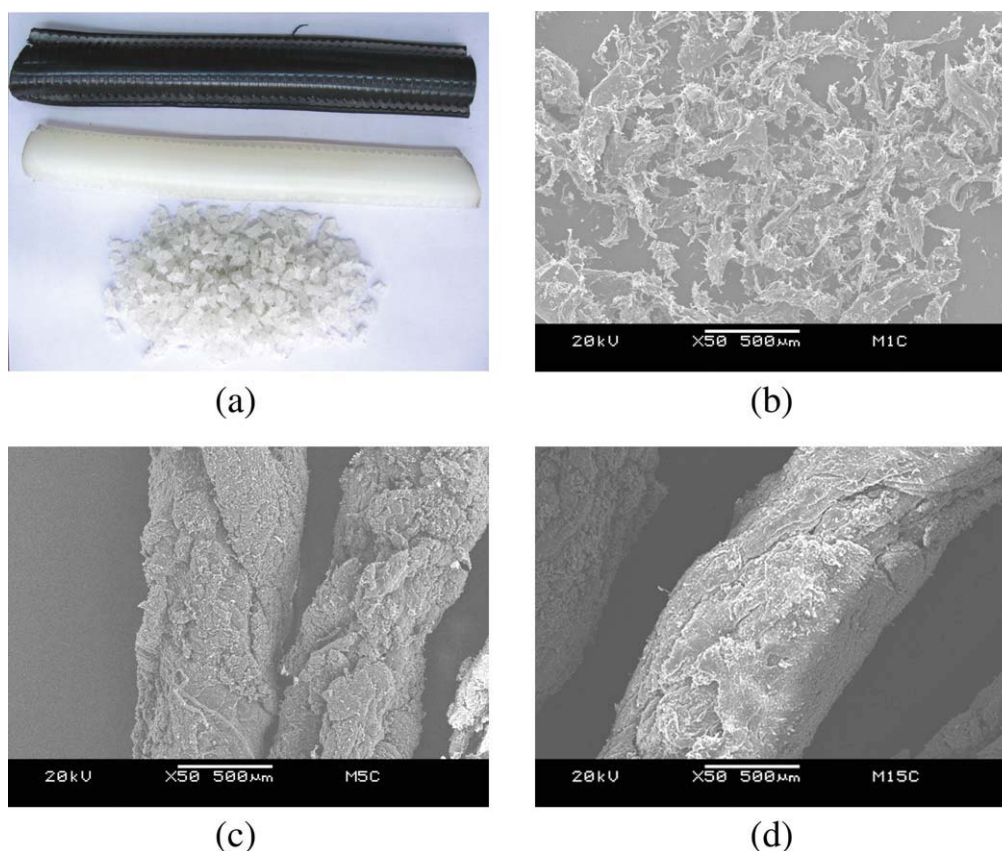


Figure 2 Digital camera picture and SEM micrographs of XLPE before and after various cycles of milling: (a) raw XLPE and its chips, (b) after 1 cycle of milling, (c) after 5 cycles of milling, and (d) after 15 cycles of milling. [Color figure can be viewed in the online issue, which is available at wileyonlinelibrary.com.]

plunger speeds after a warm-up period of 4 min. The measurements were done at a temperature of 200°C.

Mechanical properties testing

Two millimeter thick samples of the recycled XLPE with various milling cycles were compression-molded in an electrically heated hydraulic press. Hot-press procedures involved preheating at 180°C for 5 min, followed by compression for 6 min at the same temperature and at a pressure of 10 MPa and subsequent cooling under pressure for 5 min. The samples were made into dumbbell specimens, and their mechanical properties were tested at room temperature in accordance with ASTM D 412 with an Instron Universal Testing Machine (Model 5567, Instron Corporation, Canton, MA, USA) at a crosshead speed of 100 mm/min. The data were averaged over five specimens.

RESULTS AND DISCUSSION

Morphological observation of XLPE after various cycles of solid-state mechanochemical milling

The digital camera picture of the raw XLPE and its chips is shown in Figure 2(a). Its black protective jacket

of ethylene vinyl acetate (EVA) copolymers was removed first, and then, it was cut into chips of about 1 cm³ with a rotary blade chipping machine. The SEM photographs of the recycled XLPE after various mechanochemical milling cycles are shown in Figure 2(b–d). As shown clearly in the photographs, after only 1 cycle of mechanochemical milling, the XLPE chips changed into a fleecy powdery form. With increasing cycles of milling, the powdered XLPE became sticky and reunited into thin strips. Further milling was likely to generate bigger and longer strips. During mechanochemical milling, the XLPE chips were first pulverized by the strong squeezing force exerted by the pan-mill equipment, and as the cycles of milling increased, the crosslinking structure of XLPE was broken, and it could easily agglomerate to form thin strips, exhibiting better plasticity characteristics. The SEM images indicated the mechanochemical milling restored some plasticity to XLPE.

Gel fraction and SEC measurement of XLPE before and after solid-state mechanochemical milling

The realization of the restoration of plasticity due to the partial decrosslinking of XLPE was further confirmed by gel fraction measurements. Figure 3

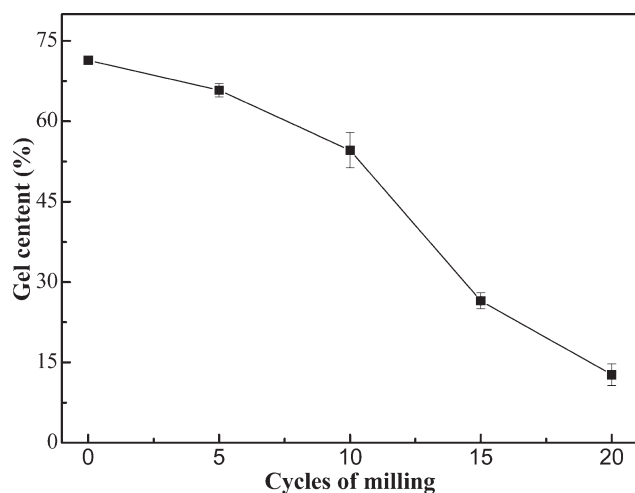


Figure 3 Effect of solid-state mechanochemical milling on the gel fraction of XLPE.

shows the effect of solid-state mechanochemical milling on the gel fraction of XLPE. It was apparent that the gel fraction correlated to the crosslinking density decreased significantly with increasing milling time from its original 70.8% to 14.5% after 20 milling cycles. This indicated that the crosslinked structure of XLPE was broken remarkably during the solid-state mechanochemical milling, which made the soluble fractions of the sample increase.

Some information relative to the breakage of the crosslinked network was indirectly revealed by the molecular characterization of the polymer fractions. In particular, soluble fractions in the raw and recycled XLPE were characterized by SEC measurements. Figure 4 shows the results of the measurements of the molecular weights of XLPE before and after 20 cycles of milling. It was evident that the sol fraction of the two samples had similar molecular weight distributions. There was a slight increase in both the weight-average molecular weight (M_w) and the number-average molecular weight (M_n) for XLPE after 20 cycles of milling; in contrast, PDI ($PDI = M_w/M_n$) became smaller compared to that of the raw XLPE. This may have been due to the partial decrosslinking occurring during mechanochemical milling; this resulted in a decrease in the polydispersity and the generation of a few constituents with molecular weights greater than 100,000.

Because the molecular weight of the sol fraction of XLPE did not decrease after milling, the significant reduction in gel fraction could be attributed to the breakage of the crosslinked structure rather than the backbone chains scission which would lead to the molecular weight reduction. The pan-mill equipment used in this study had a unique structure that could exert a fairly strong squeezing force in the normal direction and shearing force on the milled materials and function like pairs of three-dimensional scissors.

On the other hand, the crosslinking points of XLPE additionally made the chains prestressed to move physically close enough to become crosslinked; this could have also restricted the movement of the molecular chain. Therefore, when the molecular network and the entire structure was in motion during mechanochemical milling, the crosslinked structure of XLPE would most likely have had a higher opportunity for chain scissions and been broken preferably because it had the highest stress and moment.

It was clear that the crosslinking not only produced insoluble fractions but also made broader the molecular weight distribution of the soluble fractions,³² so the results of the gel fraction and SEC measurements were positive evidence that indicated that the solid-state mechanochemical milling primarily resulted in partial decrosslinking at the crosslinking points rather than the decomposition of the backbone chains.

TGA of XLPE before and after solid-state mechanochemical milling

Figure 5 shows the TGA curves for XLPE before and after 10 and 20 cycles of milling. All of the samples did not show a major weight loss up to about 420°C; beyond this temperature, a sharp weight loss was observed. However, there was still a slight increasing trend in the onset temperature of the thermal decomposition with increasing cycles of milling.

Because the crosslinking introduced tertiary carbons, which were more prone to thermal decomposition, as shown by the experimental results of refs. 33 to 35, the observed increasing trend could have been due to a reduction in the number of the tertiary carbon atoms due to partial decrosslinking. This indicated that the crosslinked structure of XLPE was broken down during mechanochemical milling. Nevertheless, these differences were almost

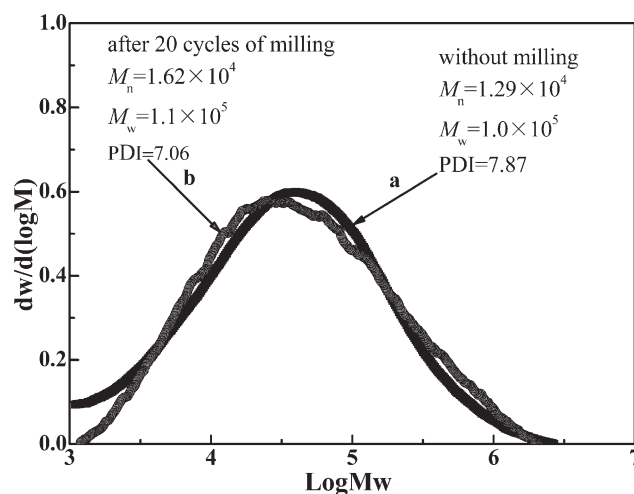


Figure 4 Molecular weight (M_w) curves of XLPE before and after 20 cycles of milling.

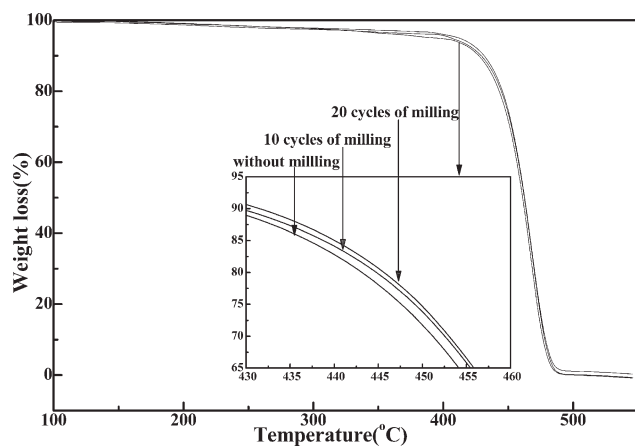


Figure 5 Effect of the cycles of milling on the thermal stability of XLPE.

negligible, and all of the polymers showed very close behavior, regardless of the gel content or cross-linking degree. This implied that the thermal stabilities of XLPE were not markedly affected by the mechanochemical milling.

Crystallinity and melting behavior of XLPE before and after solid-state mechanochemical milling

DSC was used to examine the change in the melting transitions and also the variation in ΔH_m of XLPE before and after mechanochemical milling. Figure 6 shows the DSC diagrams of XLPE before and after 20 cycles of milling, and the T_m , crystallization temperature (T_c), ΔH_m , and $X_{c,R}$, as determined from DSC measurements, are listed in Table I. The changes in crystallinity and crystallization temperature were noticeably rather small; T_m of XLPE increased from 103.5 to 107°C, and l_c increased from 5.3 to 5.9 nm. This implied that the bigger crystallites and larger average l_c formed after mechanochemical milling.

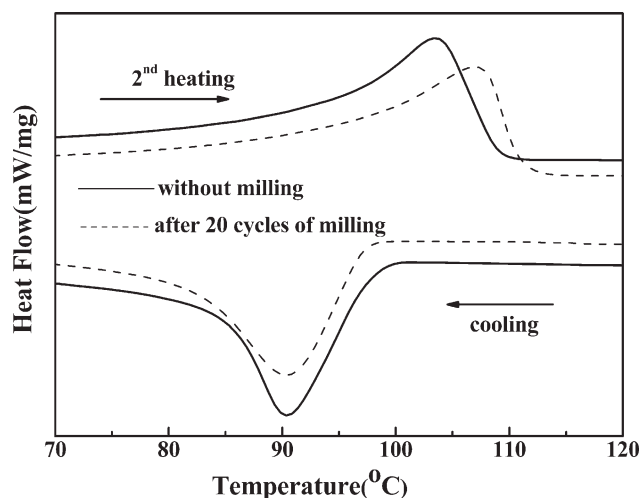


Figure 6 DSC diagrams of XLPE before and after 20 cycles of milling.

TABLE I
 T_m , ΔH_m , T_c , $X_{c,D}$, and l_c of XLPE Before and After 20 Cycles of Milling

Cycles of milling	ΔH_m (J/g)	T_m (°C)	T_c (°C)	$X_{c,D}$ (%)	l_c (nm)
0	75.2	103.5	90.3	26.9	5.3
20	76.9	107.0	90.3	27.5	5.9

As we know, crosslinks play the role of defect centers, which impede the folding of macromolecular chains and, thus, decrease the size of lamellar crystals.³⁴⁻³⁶ The solid-state mechanochemical milling led to the breakage of the crosslinked structure and then enhanced the mobility of its chain segments during the crystallization process. This resulted in the formation of a more perfect crystallite with a bigger size and an increase in l_c .

This kind of information was also confirmed by XRD analysis. Figure 7 shows the XRD scans of XLPE before and after 20 cycles of milling, and the crystal parameters calculated with the same peak separation method by the Gauss function are listed in Table II. The diffraction profiles showed typical peaks relative to the crystallographic planes (110), (200), and (020) of the orthorhombic form of PE superimposed on the amorphous halo.³⁷ The presence of these characteristic crystalline peaks clearly indicated that the crystalline structure of XLPE remained unchanged. However, the reflection (110) of the crystalline peaks of XLPE became less intensive and thinner after mechanochemical milling.

Because the reciprocal of the half-height broadening was used as a reliable parameter to evaluate both the size and perfectness of the crystallites,³⁸ as shown in Table II, the fwhm of the crystallographic plane, for instance, (110), decreased from the original 0.621 to 0.530°. This showed that the crystalline

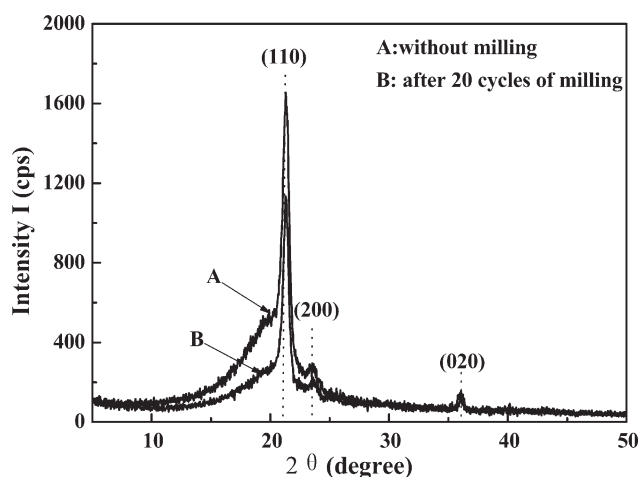


Figure 7 XRD scans of XLPE before and after 20 cycles of milling.

TABLE II
Crystal Parameters of XLPE Before and After 20 Cycles of Mechanochemical Milling

Cycles of milling	<i>hkl</i>	2 θ (°)	FWHM _{<i>hkl</i>}	Crystallite size (nm)	<i>X</i> _{<i>c,R</i>} (%)
0	(110)	21.3	0.621	15.3	25.1
	(200)	23.5	0.726	13.3	
	(020)	36.0	0.485	22.5	
20	(110)	21.4	0.530	16.7	24.6
	(200)	23.7	0.685	14.1	
	(020)	36.0	0.418	26.1	

portion increased. Meanwhile, the crystallite size increased from the original 15.3 to 16.7 nm; this showed that the crystallites became bigger and more perfect. Obviously, the parameters of the XRD pattern, such as fwhm and crystallite size, supported the results of the DSC analysis well.

Rheological and mechanical properties of XLPE after various cycles of solid-state mechanochemical milling

The flow properties of the samples studied in the molten state were analyzed by rheology. The variation of the capillary viscosity as a function of the shear rate for XLPE with various cycles of mechanochemical milling is presented in Figure 8. The curves were typical of pseudoplastic fluid behavior. It was clear that the apparent viscosities of the each sample decreased with increasing shear rate; furthermore, when the milling cycles increased, a lower apparent viscosity was observed. Such a decrease in viscosity was in accordance with the gel fraction measurement. The thermoplastic characteristic due to partial decrosslinking of XLPE during mechanochemical milling may have been responsible for the decrease in the apparent viscosity.

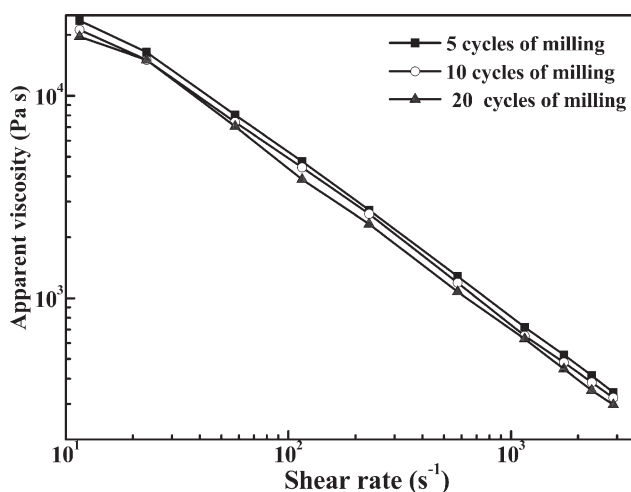


Figure 8 Rheological curves for XLPE with various cycles of milling.

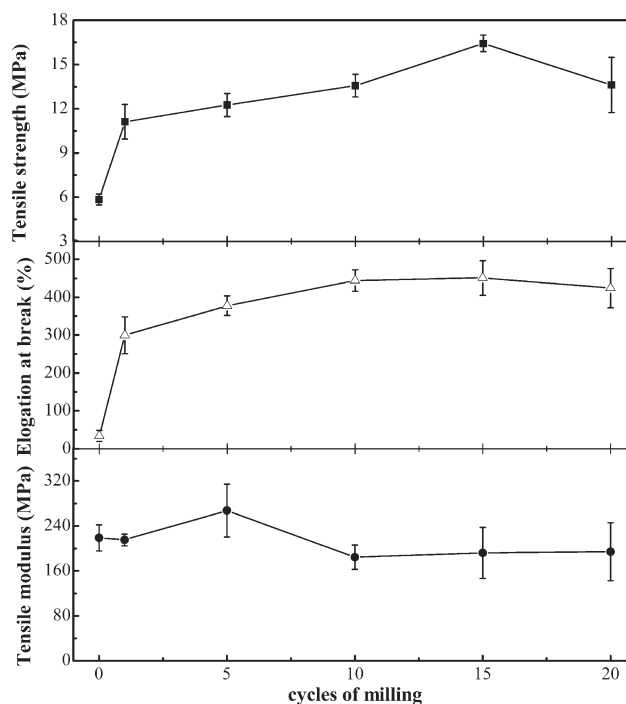


Figure 9 Effect of the milling cycles of XLPE on the mechanical properties.

The effects of the milling time on the tensile strength and elongation at break of recycled XLPE are shown in Figure 9. The specimen of raw XLPE was also obtained by hot pressing because the raw material contained about 30% soluble fractions. The tensile strength and elongation at break increased evidently with the cycles of mechanochemical milling. Also, the tensile modulus stayed almost constant; this implied that mechanochemical milling had little effect on the stiffness of the material. After 15 cycles of milling, the tensile strength increased from 5.8 to 16.4 MPa, and the elongation at break increased from 27 to 449%, about 3 times and 20 times of those of the raw XLPE, respectively. However, further mechanochemical milling seemed to have little effect on the improvement of the mechanical properties after 15 cycles of milling.

Because of the higher gel content in the raw material, chain entanglement was inadequate to form mechanically cohesive parts during melting, and many molten junctions were observed in the specimen after compression molding. This may have been the reason why this specimen showed a poor tensile strength and elongation at break. In contrast, the other specimens made from recycled XLPE could have been plasticized and, thus, were hot-pressed to continuous sheets easily; this indicated the characteristic of ease of processing. To summarize, the excellent thermoplasticity and processability of recycled XLPE, which resulted from the partial decrosslinking by mechanochemical milling, could have been the

main reason for the improvement in the mechanical properties.

CONCLUSIONS

Solid-state mechanochemical milling method was used to partially decrosslink waste XLPE to obtain a thermoplastic recycled material. The gel fraction and gel permeation chromatography measurements showed that gel content decreased remarkably with increasing cycles of milling because of the breakage of the crosslinked structure rather than the decomposition of the backbone chains. Investigation of the thermal properties showed that thermal stability slightly improved and T_m increased by 3.5°C; this was attributed to the partial decrosslinking and formation of crystallites with bigger size after mechanochemical milling. This was also confirmed by XRD analysis. SEM observation and rheological measurements indicated that the recycled XLPE exhibited improved plastic characteristics and had lower apparent viscosities; this further confirmed the occurrence of partial decrosslinking and better processability. The mechanical properties tests showed that the mechanical properties of recycled XLPE achieved a significant improvement after mechanochemical milling, and XLPE after 15 cycles of milling had the best mechanical properties in general.

All of the results indicate that solid-state mechanochemical milling enabled the waste XLPE to be a thermoplastic recycled material. Moreover, the recycling method we used in this study has advantages, such as the fact that it can be conducted at ambient temperature, is chemical free, has low energy consumption, and is more favorable for the environment.

The authors thank the Analytical and Testing Center of Sichuan University for providing the SEM and XRD measurement facilities.

References

- Bernstein, B. S. *Polym Eng Sci* 1989, 29, 13.
- Gul, R. M. *Eur Polym J* 1999, 35, 2001.
- Khonakdar, H. A.; Jafari, S. H.; Wagenknecht, U.; Jehnichen, D. *Radiat Phys Chem* 2006, 75, 78.
- Kuan, H. C.; Kuan, J. F.; Ma, C. C.; Huang, J. M. *J Appl Polym Sci* 2005, 96, 2383.
- Rafat, S.; Jamal, K.; Inderpreet, K. *Waste Manage* 2008, 28, 1835.
- Jiang, J. G.; Yang, Y.; Yang, S. H.; Ye, B.; Zhang, C. *Waste Manage* 2010, 30, 628.
- Mario, G.; Astrid, M.; Lucia, R. *Waste Manage* 2010, 30, 1238.
- Manos, M.; Yusof, I. Y.; Gangas, N. H.; Papayannakos, N. *Energy Fuel* 2002, 16, 485.
- Miskolczi, N.; Bartha, L.; Deak, G. *Polym Degrad Stab* 2006, 91, 517.
- White, C. C.; Wagenblast, J.; Shaw, M. T. *Polym Eng Sci* 2000, 40, 863.
- Achilias, D. S.; Roupakias, C.; Megalokonomos, P.; Lappas, A. A.; Antonakou, E. V. *J Hazard Mater* 2007, 149, 536.
- Toshiharu, G.; Takanori, Y.; Tsutomu, S.; Izumi, O.; Takeshi, S. *J Appl Polym Sci* 2008, 109, 144.
- Watanabe, S.; Komura, K.; Nagaya, S.; Morita, H.; Nakamoto, T.; Hirai, S.; Aida, F. In: *Proceedings of the 7th International Conference on Properties and Applications of Dielectric Material* (Nagoya, Japan; Wiley, John & Sons, Incorporated) 2003; p 595.
- Hong, S. M.; Cho, H. K.; Koo, C. M.; Lee, J. H.; Park, W. Y.; Lee, H. S.; Lee, Y. W. *Chem Eng Res* 2008, 46, 63.
- Goto, T.; Yamazaki, T. *Hitachi Cable Rev* 2004, 23, 24.
- Motonobu, G. *J Supercrit Fluid* 2009, 47, 500.
- Guo, X. Y.; Xiang, D.; Duan, G. H.; Mou, P. *Waste Manage* 2010, 30, 4.
- Xu, X.; Wang, Q. *Chin. Pat.* ZL95111258.9 (1995).
- Xu, X.; Wang, Q.; Kong, X. A.; Zhang, X. D.; Huang, J. G. *Plast Rubber Compos Process Appl* 1996, 25, 152.
- Shao, W. G.; Wang, Q.; Wang, F.; Ch, Y. H. *Carbon* 2006, 44, 2708.
- Lu, C. H.; Wang, Q. *J Mater Process Technol* 2004, 145, 336.
- Zhang, W.; Zhang, X. X.; Lu, C. H.; Liang, M. *Compos Sci Technol* 2008, 68, 2479.
- Zhang, W.; Lu, C. H.; Liang, M. *Cellulose* 2007, 14, 447.
- Liang, M.; Lu, C. H.; Huang, Y. G.; Zhang, C. S. *J Appl Polym Sci* 2007, 106, 3895.
- Zhao, B.; Lu, C. H.; Liang, M. *Chin Chem Lett* 2007, 18, 1353.
- Zhang, X. X.; Lu, C. H.; Liang, M. *Plast Rubber Compos* 2007, 36, 370.
- Zhang, X. X.; Lu, C. H.; Liang, M. *J Appl Polym Sci* 2007, 103, 4087.
- Zhang, X. X.; Lu, C. H.; Liang, M. *J Polym Res* 2009, 16, 411.
- Krupa, I.; Luyt, A. S. *J Appl Polym Sci* 2001, 81, 973.
- Hosoda, D. *Polym J* 1988, 20, 383.
- Khonakdar, H. A.; Jafari, S. H.; Taheri, M.; Wagenknecht, U.; Jehnichen, D.; Haussler, L. *J Appl Polym Sci* 2005, 100, 3264.
- Gabriella, C.; Vincenzo, V.; Liana, A.; Stefania, P.; Pasquale, L.; Gaetano, G. *Polymer* 2005, 46, 2847.
- Krupa, I.; Luyt, A. S. *Polym Degrad Stab* 2000, 70, 111.
- Khonakdar, H. A.; Morshedjan, J.; Wagenknecht, U.; Jafari, S. H. *Polymer* 2003, 44, 4301.
- Marcilla, A.; Ruiz-Femenia, R.; Hernandez, J.; Garcia-Quesada, J. C. *J Anal Appl Pyrol* 2006, 76, 254.
- Mtshali, T. N.; Krupa, I.; Luyt, A. S. *Thermochim Acta* 2001, 380, 47.
- Paola, R.; Francesca, B.; Gaetano, G. *Macromolecules* 2001, 34, 5175.
- Vittoria, V. J. *J Macromol Sci Phys* 1989, 28, 489.